Stable isotopes track the ecological and biogeochemical legacy of mass mangrove forest dieback in the Gulf of Carpentaria, Australia

Yota Harada[1], Rod M. Connolly[1], Brian Fry[2], Damien T. Maher[3,4], James Z. Sippo[3], Luke C. Jeffrey[3], Adam J. Bourke[5], Shing Yip Lee[6]

5   [1]Australian Rivers Institute – Coast and Estuaries, and School of Environment and Science, Griffith University, Gold Coast, Queensland, Australia
[2]Australian Rivers Institute, Griffith University, Nathan, Queensland, Australia
[3]Southern Cross Geoscience, Southern Cross University, Lismore, New South Wales, Australia
[4]School of Environment, Science and Engineering, Southern Cross University, Lismore, NSW, Australia
10 [5]College of Engineering, Information Technology and the Environment, Charles Darwin University, Northern Territory, Australia
[6]Simon F.S. Li Marine Science Laboratory, School of Life Sciences, and Earth System Science Programme, The Chinese University of Hong Kong, Shatin, Hong Kong SAR, China

Correspondence to: Yota Harada (yota.harada@griffithuni.edu.au)

15 **Abstract.** A combination of elemental analysis and stable isotope analysis (SIA) was used to assess and monitor C, N and S cycling of a mangrove ecosystem that suffered mass dieback of trees in the Gulf of Carpentaria, Australia in 2015-16, attributed to an extreme drought event. Three field campaigns were conducted over a period from 2016 to 2018, at 8, 20 and 32 months after the event. Samples including invertebrates, mangroves, and sediment were analysed for CNS elemental and isotopic compositions including compound-specific stable isotope analysis (CSIA) of amino acid carbon. Samples collected 20 from the impacted ecosystem were enriched in ^{13}C, ^{15}N and ^{34}S relative to those from an adjacent unimpacted reference ecosystem, likely indicating lower mangrove carbon fixation, lower nitrogen fixation and lower sulfate reduction in the impacted ecosystem. For example, invertebrates representing the feeding types of grazing, leaf feeding, and algae feeding were more ^{13}C enriched at the impacted site, by 1.7 – 4.1‰ and these differences did not change over the period from 2016 to 2018. The CSIA data indicated widespread ^{13}C enrichment across five essential amino acids and all groups sampled 25 (except filter feeders) within the impacted site. Mangrove seedling and sapling populations increased substantially from 2016 to 2018 in the impacted forest, suggesting recovery of the mangrove vegetation. Recovery of CNS cycling, however, was not evident even after 32 months, suggesting a biogeochemical legacy of the mortality event. Continued monitoring of the post-dieback forest would help to predict the long-term trajectory of ecosystem recovery. In such long-term monitoring programs, SIA that can track biogeochemical changes over time can help to detect underlying biological mechanisms that drive 30 changes and recovery of the mangrove ecosystem. To gain further insight, our use of CSIA can help show feeding dependencies in mangrove food webs and their response to disturbances.

1 Introduction

Stable isotope analysis (SIA) is a powerful tool for environmental assessment and monitoring that provides information about biogeochemical source and processes over time. As elements such as carbon (C), nitrogen (N) and sulfur (S) circulate

35 in the biosphere, stable isotopic compositions of $^{13}C/^{12}C$, $^{15}N/^{14}N$ and $^{34}S/^{32}S$ change in predictable ways due to mixing and fractionation, giving insights into sources and cycling of these elements (Fry 2006). SIA has been widely used in mangrove ecosystem studies to better understand food web interactions (Bouillon et al., 2008; Larsen et al., 2012; Bui and Lee, 2014; Abrantes et al., 2015), mangrove nutrient uptake (McKee et al., 2002), mangrove water use (Santini et al., 2015; Hayes et al., 2019), cycling of C (Maher et al., 2013a; Maher et al., 2017; Sasmito et al., 2020), N (Fry and Cormier, 2011), S (Raven et

40 al. 2019), and greenhouse gas emissions (Maher et al., 2013b).

Low frequency, high intensity weather events, such as droughts, tropical cyclones, heatwaves and climatic extremes can cause mass mortality of foundation species such as mangroves (Sippo et al., 2018), saltmarshes (Silliman et al., 2005), seagrasses (Thomson et al., 2015), kelps (Wernberg et al., 2016) and corals (Hughes et al., 2017). The frequency and

45 intensity of extreme climatic events are expected to increase due to climate change (Coumou and Rahmstorf, 2012; Stott, 2016). In 2015-16, an extensive area (>7000 ha) of mangrove forest along ~1,000 km of coastline in the Gulf of Carpentaria, Australia, experienced severe dieback, an event associated with the climatic extreme of drought (Duke et al., 2017). As mangroves show characteristics of pioneer species (Tomlinson, 2016), large-scale disturbances have likely played an important role in their evolution. However, the processes, rates and patterns of recovery from disturbances are still largely

50 unknown. In most cases, recovery of mangroves primarily relies on the recruitment of seedlings (Smith et al., 1994; Krauss and Osland, 2019). Disturbances in mangrove forests not only affect recruitment, but can also change the cycling of C, N and S. Loss of mangrove trees and root structures can change organic matter inputs, sediment oxygenation and degradation of sediment organic matter. These changes alter overall sediment conditions, with consequences for benthic assemblages (Sweetman et al., 2010; Bernardino et al., 2018; Harada et al., 2019), sediment C and N stocks (Adame et al., 2018),

55 microbial assemblages, and associated nutrient processes e.g. nitrogen fixation and sulfate reduction (Sjöling et al., 2005).

Traditional methods to evaluate structure and functioning of ecosystems include measures of species composition, but these field assessments can be time-consuming and expensive and may not provide enough quantitative information about system functioning (e.g. Kling et al.,1992). SIA of ecosystem components is a powerful way of quantitatively evaluating functional

60 aspects of element cycling and the health of ecosystems (e.g. integrity of the food web; Fry, 2006). SIA of total organic matter (''bulk'') have become widespread due to the relative ease and low cost of sample preparation and analysis (Fry, 2006). Compound-specific stable isotope analysis (CSIA) is increasingly employed as a complementary tool to bulk SIA. For instance, while bulk SIA of C, N and S provide an overview of food webs (Bouillon et al., 2008), CSIA of amino acids (AAs) help measure details of organic matter cycling (Ishikawa et al., 2018; Larsen et al., 2013; Ohkouchi et al., 2017)

65

We investigated changes in C, N and S cycling associated with the Gulf of Carpentaria mangrove forest dieback (Duke et al., 2017), using a combination of traditional ecological survey techniques, bulk SIA, and CSIA of amino acid carbon. We hypothesised that the mortality of mangrove foundation species has changed the overall circulation of C, N and S elements and these biogeochemical changes would most likely be reflected in $\delta^{13}C$, $\delta^{15}N$ and $\delta^{34}S$ values of mangrove ecosystem

70   components such as mangrove plants, sediment and associated animals. We also tested the hypothesis that these isotopic compositions changed over time with the recovery of mangrove vegetation. $\delta^{13}C$, $\delta^{15}N$ and $\delta^{34}S$ values were measured for samples including mangroves, sediment and invertebrates collected in a comparative setting of impacted mangrove forest site and an adjoining unaffected reference forest site in the Gulf of Carpentaria, Australia.

2 Material and Methods

75   ### 2.1 Study site

Over 7,000 ha of mangroves along ~ 1,000 km of the Gulf of Carpentaria coastline in Australia experienced mass mortality during the summer in 2015-16, (Duke et al., 2017), the most extensive mangrove forest dieback ever recorded due to natural causes (Sippo et al., 2018). At the same time, there were coinciding mangrove mass mortality events in Exmouth, Western Australia (Lovelock et al., 2017) and Kakadu National Park, Northern territory (Asbridge et al., 2019). The climate in the

80   Gulf region is wet-dry tropical with mean annual precipitation ranging from approximately 600 to 900 mm. Dry conditions prevail for six to eight months and most rainfall occurs between December and March (Bureau of Meteorology, see www.bom.gov.au). The climatic conditions limit the extent of mangroves in the region (Asbridge et al., 2016). The dieback was most likely linked to a weak monsoon (low rainfall), combined with high vapor pressure deficit, and El Niño–Southern Oscillation-induced low sea-levels (Duke et al., 2017; Lovelock et al., 2017; Harris et al., 2017; Harris et al., 2018). These

85   conditions most likely resulted in hypersalinization and caused accumulative hydric, thermal and radiant stresses (Duke et al., 2017; Lovelock et al., 2017; Harris et al., 2017; Harris et al., 2018). The event led to the widespread death of mangrove trees in the region providing a unique opportunity to test tree mortality effects on biogeochemical and ecological functioning of mangroves and capture recovery patterns.

90   Three field campaigns were conducted in August 2016 (8 months after the event), August 2017 (20 months after the event) and August 2018 (32 months after the event) in the winter dry-seasons in Karumba, Gulf of Carpentaria, Australia (Fig. 1A). Some local factors (e.g. river influence) may have kept some mangroves from dying back in the region. A forest that had suffered dieback (impacted) on the east of Norman river outlet and an adjoining unaffected forest (unimpacted) on the west, provided the setting for comparisons. *Avicennia marina* was the dominant mangrove species. In order to assess differences

95   between the two forests (impacted vs. unimpacted), as well as to capture trends from across the intertidal zone and to ensure that the physical-oceanographic conditions between the two forests were as similar as possible, three sampling transects (2 to

2.5 km apart) were set for each forest with the length of each transect being approximately 200 m (Fig. 1B, C). Due to logistical constraints and the presence of saltwater crocodiles, fieldwork was restricted to daytime, low tide and dry seasons.

2.2 Samples

100 Three field campaigns were carried out in August 2016, 2017 and 2018. Since our focus was to measure recovery of mangrove vegetation and food-web, we monitored mangrove sapling/seedlings and stable isotopes of invertebrates during the period from 2016 to 2018. Mangrove and sediment samples were also collected but they are limited to 2018 (Table 1). Some of the SIA samples including invertebrates, mangrove and sediment collected in 2017 were used to measure the initial dieback reported in Harada et al. (2019).

105

During each field campaign, four common mangrove macroinvertebrate groups with different feeding modes were collected from each forest including a leaf-eating crab (*Parasesarma molluccensis* and/or *Episesarma* sp.), an algae-eating (deposit-feeding) crab (*Tubuca signata*), a grazer gastropod (*Telescopium telescopium*) and a filter-feeding bivalve (*Saccostrea sp,* an oyster). For each feeding group, 3 to 5 individuals at each of the sampling transects (n=3) within the forest were collected

110 and muscle tissues were pooled for SIA.

In 2018, we further divided each transect into five zones (50m apart), namely forest edge (landward), high, mid, low and forest edge (seaward). Fully developed green leaves of *A. marina* were collected from at about 1 to 1.5 m height, from 3 to 5 individual trees (1 to 3 leaves per tree) at each zone, stored in plastic containers, then composited. In the impacted site,

115 regrowth was occurring in some trees, and leaves were collected from this regrowth. Leaf samples were washed thoroughly, rinsed with distilled water and the main vein was removed. Additionally, wood samples (n=2) were collected from each forest. Two to three bulk SIA measurements were made for each wood sample and measurements were averaged. Wood samples were generally very low in S and only one wood sample had sufficient S for $\delta^{34}S$ analysis.

120 In 2018, surface (<0.5 cm) sediment was collected along the intertidal zones of each transect from the forest edge (landward) to forest edge (seaward) and also in the adjacent mudflat. Additionally, in each forest, 0.5 to 20 cm sediment samples (n=6) were collected using a core sampler, 5 cm in diameter and 20 cm deep. For $\delta^{13}C$ measurements, the sediment samples were acidified with 1M HCl to remove the inorganic fraction. Microphytobenthos (MPB) samples (n=6) were separated from surface sediment collected at each forest. The separation was achieved through density gradient centrifugation in Ludox

125 colloidal silica (Sigma) as described in Bui and Lee (2014). The MPB extraction was followed by microscopic examination to confirm that samples mostly contained green cells (i.e. diatoms and filamentous cyanobacteria). Additionally, surface sediment samples were collected from offshore (approx. 1km) using a grab sampler and from the adjacent saltpan (approx. 200m inland from the forest). Offshore water samples (n=3) were also collected and then filtered through glass fiber filters (diameter 44mm, pore size 0.7μm, Whatman GFF) to obtain particulate organic matter (POM).

130

To estimate mangrove seedling/sapling densities (ind. m^{-2}) from each forest and their changes over the two-year period (2016 to 2018), seedling/saplings were counted with 50 x 50 cm quadrats. In this process, photographs were taken in the field (for 2016, n=124 for the unimpacted forest and n=143 for the impacted forest, for 2017, n=161 and n=175, and for 2018, n=80 and n=17, respectively) and then counts of seedlings and samplings were made in the laboratory. The

135   seedlings/samplings were mostly *A. marina* but also include some *Aegiceras corniculatum*.

2.3 Stable isotope analysis

All invertebrate, leaf, sediment and filter samples were stored separately in sealed plastic containers at -20°C until analysis, then dried at 60°C, powdered, homogenized and put in tin capsules for SIA. $\delta^{13}C$, $\delta^{15}N$ and $\delta^{34}S$ measurements were carried out on an elemental analyzer (Europa EA-GSL, Sercon) coupled to an isotope ratio mass spectrometer (Hydra 20-22,

140   Sercon) at Griffith University, Brisbane, Australia. Isotope values are reported relative to Vienna Pee Dee Belemnite (PDB), atmospheric N$_2$ (AIR), and Vienna Canyon Diablo Troilite (VCDT) for C, N and S, respectively. Harada et al. (2019), reported $\delta^{13}C$ and $\delta^{15}N$ values for some of the samples collected in 2017 from the same study location.

The samples collected in 2017 showed substantial differences in $\delta^{13}C$ values between the two forests (Harada et al., 2019)

145   suggesting that they are representative of the dieback impact. The 2017 samples from each forest including the mangrove leaf (n=2), MPB (n=1), algae feeder (n=3), leaf feeder (n=2 to 3), grazer (n=3), filter feeder (n=2) were further measured for carbon isotopic composition of individual amino acids ($\delta^{13}C_{AA}$). For this CSIA, 8 mg (for animal tissues) or 30 mg (for plant tissues) of sample materials were transferred to borosilicate vials with heat and acid-resistant caps. They were then flushed with N$_2$ gas, sealed and hydrolysed in 0.5mL (animal tissues) or 2mL (plant tissues) of 6M HCl at 150°C for 70 minutes,

150   then dried in a heating block at 60°C under a stream of N$_2$ gas. The dried samples were derivatised by methoxycarbonylation as described by Walsh et al. (2014). Amino acid derivatives were separated by a Trace GC Ultra gas chromatograph (Thermo Scientific) using a DB-23 column, Agilent, 30m x 0.25mm, 0.25µm film at the stable isotope facility at the University of California (Davis, CA, USA). The GC was interfaced with a Delta V Plus isotope ratio mass spectrometer via a GC IsoLink (Thermo Scientific). L-Norleucine was used as an internal standard and to calculate provisional values.

155

Pure AAs mixtures with calibrated $\delta^{13}C$ were co-measured. One mixture was used for final calibration and others were for the scale normalisation standard and the primary quality assurance standard (unused in corrections). Two working standards were co-measured as secondary quality assurance materials. Exogenous carbon was accounted by the method detailed by Docherty et al. (2001). Following these processes, $\delta^{13}C$ values were determined for 10 AAs (Gly, glycine; Asx, aspartic

160   acid/asparagine; Pro, proline; Glx, glutamic acid/glutamine; Ala, alanine; Lys, lysine; Ile, isoleucine; Leu, leucine; Phe, phenylalanine; and Val, valine). Met, methionine; His, histidine; and Hyp, hydroxyproline were at or below the limit of

quantitation (LOQ) for some samples. Since we were interested in $\delta^{13}C$ values of essential amino acids ($\delta^{13}C_{EAA}$), we only report $\delta^{13}C$ values of Lys, Ile, Leu. Phe and Val.

2.4 Data analysis

165 All statistical analyses were undertaken in R version 3.4.3 with RStudio interface version 1.1.414. Differences among group means were explored with ANOVA, but for the count data i.e. seedling/ sampling populations, generalized linear model (GLM) with Poisson distribution was used. Before performing ANOVA, the assumptions of homogeneity of variance and normality were tested using Levene's and Shapiro-Wilk's tests, respectively. Two way ANOVA was used to test the effects of time (year) and forest type (unimpacted and impacted) on stable isotope values of invertebrates. To explore $\delta^{13}C$ patterns

170 among five EAAs, $\delta^{13}C_{EAA}$ values were normalised to the respective sample means following the procedure of Larsen et al. (2009) as follows:

$$Norm(\delta_{EAA}) = \delta_{EAA} - \mu \qquad\qquad (1)$$

where μ represents the mean value of all five EAAs (Ile, Leu, Lys, Phe and Val) in the sample. PERMANOVA was performed to test if the pattern of $\delta^{13}C$ among five EAAs of samples differ between the forests. In this analysis, the

175 normalized $\delta^{13}C_{EAA}$ dataset was used and the Euclidean distance was used as distance metric. Permutation test of multivariate homogeneity of dispersions was performed to check whether dispersions around the centroids are similar between the two forests. All statistical tests used a significance criterion of α=0.05.

3 Results

3.1 Mangroves

180 In 2016, approx. 8 months after the mangrove mortality event, at the impacted site, mangrove seedling and sapling populations were lower than the unimpacted site (GLM df = 1, estimate 3.75, p < 0.001) but significantly increased throughout the period from 2016 to 2018 (GLM df = 2, estimate 0.01, p < 0.001; Fig. 2). C, N and S elemental compositions (%) of the dominant mangrove species, *A. marina* did not differ greatly between the two sites, but the isotopic compositions varied considerably in 2018 (32 months after the dieback; Table 2). The $\delta^{13}C$ values (mean ± SD) of green leaves harvested

185 from *A. marina* trees, were significantly higher (i.e. more ^{13}C-enriched) in the impacted site (-25.8 ± 1.0‰) than the unimpacted site (-28.4 ± 1.5‰; ANOVA $F_{1, 28}$ = 32.9, p < 0.001; Fig. 3A, Table 2). The $\delta^{15}N$ values varied more in the impacted site (ranged from -0.9 to 6.7‰) than in the unimpacted site (ranged from 2.9 to 6.2‰; Fig. 3A). The $\delta^{34}S$ values were generally higher in the impacted site (13.5 ± 5.4‰, range 7.7 to 23.3‰) than the unimpacted site (12.6 ± 5.6‰, range 5.0 to 21.9‰). Leaf $\delta^{34}S$ values became more ^{34}S depleted from higher to lower intertidal zones in the impacted site

190 (ANOVA $F_{4, 10}$ = 5.56, p = 0.013; Fig. 3B). This pattern was weaker in the unimpacted site, but leaf $\delta^{34}S$ values substantially varied across intertidal zones (ANOVA $F_{4, 10}$ = 6.48, p = 0.007; Fig. 3B). Leaf $\delta^{13}C$ and $\delta^{15}N$ values did not display such

patterns along the intertidal zones. Leaf C, N and S (%) did not show any clear trends among two forests and along transects. Yellow leaves generally had a higher S content (~1.2%) than green leaves (0.5 to 0.7%) (Table 2). Wood samples generally had very low N and S contents, significantly lower than the leaves. However, wood samples from the impacted site had a

195 relatively high S content (0.31 ± 0.37%) and had a $\delta^{34}S$ value of 16.6‰ (Table 2).

3.2 Sediment

For the surface (0 - 0.5 cm) sediment collected in 2018 (32 months after the dieback), TOC (%) differed significantly between the two forests with the values (mean ± SD) of 2.02 ± 1.16% for the unimpacted site and 1.06 ± 0.37% for the impacted site (ANOVA $F_{1, 28}$ = 12.75, P = 0.001), suggesting that the surface sediment from the impacted site contains ~48%

200 lower TOC relative to those of the unimpacted site (Table 3). The pattern was consistent across the intertidal zones (Fig 4A). The surface sediment TN (%) was also significantly lower for the impacted site (0.09 ± 0.03) than the unimpacted site (0.15 ± 0.06%; ANOVA $F_{1, 28}$ = 9.32, P = 0.005). TOC of mudflat (<0.5 cm) sediment collected adjacent to the two forests also differed significantly with those of impacted site being lower (0.58 ± 0.18%) than the unimpacted site (1.02 ± 0.08%; ANOVA $F_{1, 4}$ = 14.54, P = 0.019). TN (%) of mudflat (<0.5 cm) sediment was also significantly lower for the impacted site

205 (ANOVA $F_{1, 4}$ = 9.81, P = 0.035). TOC (%) of 0.5 – 20 cm sediment did not differ significantly between the two sites with the values of 1.83 ± 0.73% for the unimpacted and 1.29 ± 0.55 % for the impacted site (ANOVA $F_{1, 10}$ = 2.07, P = 0.181). TN (%) of 0.5 – 20 cm sediment also did not differ significantly between the two sites with the values of 0.09 ± 0.03% for the unimpacted and 0.12 ± 0.04% for the impacted site (ANOVA $F_{1, 10}$ = 3.02, P = 0.113).

210 The $\delta^{13}C$ values of surface (< 0.5 cm) sediment differed significantly between the two sites with those from the impacted site showing higher values (-21.8 ± 1.0‰) than the unimpacted site (-24.3 ± 1.2‰; ANOVA $F_{1, 28}$ = 22.48, P < 0.001). This pattern was consistent across the intertidal zones with $\delta^{13}C$ values from the impacted site becoming similar to those from the adjacent mudflat (Fig. 4b). However, those of 0.5 to 20 cm sediment did not differ significantly with the values of -24.4 ± 0.5‰ for the impacted site and -25.2 ± 0.9‰ for the unimpacted site (ANOVA $F_{1, 10}$ = 3.92, P = 0.076). Surface (< 0.5 cm)

215 sediment collected in the adjacent mudflat did not display a significant difference in $\delta^{13}C$ values between the two sites with the values of -21.2 ± 0.9‰ for those collected adjacent to the unimpacted forest and -21.8 ± 0.8‰ for those collected adjacent to the impacted site (ANOVA $F_{1, 4}$ = 0.64, P = 0.47). The $\delta^{13}C$ value of the surface sediment (-21.8 ± 1.0‰) in the impacted forest was similar to those collected in the mudflat (-21.2 ± 0.9‰) which were also similar to those collected from offshore (-21.8 ± 1.1‰). Those $\delta^{13}C$ values also matched with the $\delta^{13}C$ value of POM collected offshore (-21.5 ± 1.5‰).

220 Surface (< 0.5 cm) sediment collected from adjacent unvegetated saltpan areas also showed similar values (Table 3). MPB extracted from the surface <0.5 cm sediment showed significantly different $\delta^{13}C$ values between the impacted site (-21.5 ± 1.3‰) and unimpacted site (-25.2 ± 1.0‰; ANOVA $F_{1, 10}$ = 28.53, P < 0.001).

3.3 Fauna

CNS isotopic compositions of mangrove macroinvertebrates representing algivores, grazers and leaf feeders from the
225 impacted site were consistently more enriched in ^{13}C, ^{15}N and ^{34}S than their counterparts from the unimpacted forest
throughout the period between 2016 and 2018 (Fig. 5). However, the filter feeding oyster that relies on water column organic
matter showed relatively less differences between the two forests (Fig. 5). Overall, δ^{13}C values of the four feeding groups
range from -23 to -15‰ for the unimpacted site and -20 to -14‰ for the impacted site. The δ^{15}N values ranged from 5.5 to
9.1‰ for the unimpacted site with the fauna in the impacted site having a slightly higher range of 5.6 to 9.5‰. The δ^{34}S
230 values ranged from 8.2 to 16‰ for the unimpacted site and 13.4 to 21.7‰ for the impacted site. The effect of forest type was
significant for δ^{13}C, δ^{15}N and δ^{34}S values of the algae feeder and the grazer (ANOVA p < 0.05). The effect of forest type was
also significant for δ^{13}C and δ^{34}S values of the leaf feeder (ANOVA p < 0.05), but was not significant for the δ^{15}N values
(ANOVA $F_{1, 13}$ = 1.72, p = 0.212). The effect of forest type was not significant for the filter feeder δ^{13}C values (ANOVA $F_{1, 8}$
= 1.719, p = 0.212), but was significant for the δ^{15}N and δ^{34}S values (ANOVA p < 0.05). The effect of time was significant
235 for the leaf feeder δ^{34}S values, the grazer δ^{15}N values, the filter feeder δ^{15}N and δ^{13}C values (ANOVA p < 0.05). Overall, the
δ^{13}C, δ^{15}N and δ^{34}S values of mangrove invertebrates consistently differed between the sites during the period from 2016 to
2018. In 2018, leaf feeder δ^{13}C values, grazer δ^{34}S values and algae feeder δ^{34}S values significantly differed between the
impacted and unimpacted sites (Turkey post hoc test, P < 0.05), showing no recovery of the invertebrate fauna δ^{13}C and δ^{34}S
status after 32 months from the dieback event. However, δ^{15}N values started showing matches between the two forests in
240 2018 (Fig. 5).

3.4 Compound-specific isotope analysis of amino acid carbon

The samples collected in 2017 were further measured for carbon isotopic compositions in individual essential amino acids.
$\delta^{13}C_{EAA}$ values corresponded to the bulk δ^{13}C values with the samples from the impacted site consistently showing higher
values than those from the unimpacted forest (Table 4 and Fig 6). The pattern of δ^{13}C among five EAAs (Lys, Ile, Val, Leu
245 and Phe) for all the consumers did not differ between the two forest types (p > 0.05; Table 4 and Fig S1), including the
algae-feeder, leaf feeder, grazer and filter feeder. The $\delta^{13}C_{EAA}$ pattern of mangrove leaves did not differ between the forests,
regardless of the substantial bulk isotope difference between the unimpacted (-26.7 ± 2.2‰) and impacted (-25.4 ± 0.1‰)
(Table 4). This isotope pattern was similar for all four feeding groups as well as for the MPB samples (Fig. 6 and Fig S1).

4. Discussion

250 **4.1 Mangroves**

The recovery of mangrove forests from tree mortality events caused by disturbances such as cyclones, generally relies upon the recruitment of seedlings (Smith et al., 1994; Krauss and Osland, 2019). Subsequently, degraded habitats with a reduced seed pool, production and delivery, e.g. by habitat fragmentation, may show slower forest recovery (Milbrandt et al., 2006). The establishment of seedlings may also be inhibited by persistent inundation due to a decreased sediment elevation (Cahoon

255 et al., 2003; Asbridge et al., 2018). Although mangroves are resilient ecosystems and may recover quickly from natural disturbances (Sherman et al., 2001), in some cases recovery may take more than 10 years (Imbert et al., 2000). Further, mangrove degradation may be followed by fast colonisation of non-mangrove herbaceous species (McKee et al., 2007; Rashid et al., 2009), e.g. succulent saltmarsh (Mbense et al., 2016). In the impacted Gulf of Carpentaria mangrove forest, the density of mangrove seedling/samplings significantly increased throughout the period from 2016 to 2018, suggesting that

260 recovery is starting to occur in some areas within 32 months after the dieback (Fig. 2).

The substantial differences in CNS isotopic compositions in *A. marina* occurring between the two sites, suggested differences in the environmental conditions and biogeochemical processes that were possibly associated with the mangrove mortality effect. The leaf $\delta^{13}C$ values in the impacted forest were relatively enriched in ^{13}C. This C isotope pattern may be

265 due to reduced stomatal conductance that causes lower internal carbon dioxide concentrations and lower carbon isotope fractionation (Farquhar et al., 1989; Lin and Sternberg, 1992a; Lin and Sternberg, 1992b). ^{13}C-enriched leaf $\delta^{13}C$ values can also be associated with increased carboxylation efficiency associated with higher nutrients, .e.g. N in leaves (Cordell et al., 1999) and thicker leaves with higher internal resistance to carbon dioxide diffusion. Younger leaves can show higher $\delta^{13}C$ values than aged leaves due to ^{13}C enriched fractions (e.g. carbohydrates) transported from older autotrophic leaves to more

270 heterotrophic young leaves (Werth et al., 2015). Leaves exposed to full sun can show higher $\delta^{13}C$ values than shaded leaves (Farquhar et al., 1989). $\delta^{13}C$ values can vary among different plant tissues in *A. marina* (Kelleway et al., 2018). Leaf N (%) did not differ between the two forests, suggesting that the two sites may have similar plant N availability. Previous studies show additions of nutrients such as N and/or P did not play a considerable role in mangrove leaf $\delta^{13}C$ variations (McKee et al., 2002), but salinity played an important role (Lin and Sternberg, 1992b). For example, leaf $\delta^{13}C$ values of *A. marina* at a

275 lower salinity site was relatively depleted in ^{13}C and averaged about -31‰ (Kelleway et al., 2018). Overall, ^{13}C-enriched leaf $\delta^{13}C$ values in the impacted forest likely suggest that there are chronic stresses associated with the dieback event that reduced stomatal conductance. Such environmental stresses may include hypersalinization of sediments and hydric, thermal and radiant stresses following mangrove losses (e.g. canopy loss).

280 Leaf $\delta^{15}N$ values varied more in the impacted (ranged from -0.9 to 6.7‰) than in the unimpacted forest (ranged from 2.9 to 6.2‰) (Fig. 3), but the means were similar (4.3 ± 1.9‰ for the impacted and 4.4 ± 0.8‰ for the unimpacted), suggesting

that two sites have similar background $\delta^{15}N$ conditions. Generally, leaf $\delta^{15}N$ varies due to N sources, microbial processes that enrich or deplete ^{15}N in soil or water, and isotope fractionation during plant N uptake. Previous studies showed that in pristine mangrove forests, leaf $\delta^{15}N$ values generally range around -2‰ to 3‰ (Fry and Smith, 2002; Smallwood et al., 2003). Such low $\delta^{15}N$ values may reflect long-term N fixation inputs (e.g. around 0‰) (Fogel et al., 2008) and marine nitrate inputs (Dore et al., 2002). Much higher $\delta^{15}N$ values (>10‰) may be associated with anthropogenic N inputs (Fry and Cormier, 2011). Our sites showed moderate $\delta^{15}N$ values (about 4‰), suggesting that in addition to N fixation inputs and marine N inputs, there may be considerable microbial ^{15}N enrichment in dissolved inorganic nitrogen pools of ammonium and nitrate. The higher variability in leaf $\delta^{15}N$ in the impacted forest suggests higher variability in processes affecting the $\delta^{15}N$ status of available N. For example, changes to sediment conditions following the dieback affected microbial processes of N, whereas the unimpacted forest has more stable N pool, processes and inputs. Isotope fractionation during plant N uptake may also be an explanation for leaf $\delta^{15}N$ variability (Fry et al., 2000), but such fractionation is poorly known for mangroves. A study reported that additions of P nutrients increased N demand and decreased ^{15}N fractionation (McKee et al., 2002), however as we did not measure P, we could not determine whether this was the case.

Leaf $\delta^{34}S$ values differed considerably between the two forests, with the impacted forest generally having higher values (13.5 ± 5.4‰, range 7.7 to 23.3‰) than the unimpacted forest (12.6 ± 5.6‰, range 5.0 to 21.9‰). Leaf $\delta^{34}S$ values showed trends along the six transects, with values decreasing from the upper to lower intertidal zones (Fig. 3B). Based on previous studies, mangrove leaf $\delta^{34}S$ values generally vary between -20 to 20‰ (Okada and Sasaki, 1995, 1998; Fry and Smith, 2002). Higher $\delta^{34}S$ values are likely associated with seawater sulfate, which is ^{34}S enriched (i.e. 21‰) and due to a large isotope fractionation (up to 70‰) during sulfate reduction (Kaplan and Rittenberg, 1964). Lower $\delta^{34}S$ values are likely associated with sedimentary sulfide-S that is ^{34}S depleted, for example, -21‰ (Okada and Sasaki, 1995). Leaf $\delta^{34}S$ values of around 14 to 18‰ suggest mangrove incorporations of seawater sulfate-S ($\delta^{34}S$, ~ 21‰), with only a small isotopic fractionation occurring through absorption and assimilation steps (Okada and Sasaki, 1995). Plants generally show $\delta^{34}S$ values slightly lower than source sulfate-S by an average of -1.5‰ (Trust and Fry, 1992). Low leaf $\delta^{34}S$ values, for instance, the lowest value of 5‰ found in the unimpacted site - suggest that the most probable source of this ^{34}S-depleted S is sulfide oxidation, followed by mixing with seawater sulfate. Low $\delta^{34}S$ values in mangrove root vascular tissues may indicate assimilation/oxidation of sulfide, potentially to reduce their toxic sulfide exposure (Fry et al., 1982; Raven et al., 2019), with reported isotope effect of -5.2‰ for non-biological oxidation of sulfide (Fry et al., 1988) and a smaller +1-3 ‰ effect for anaerobic oxidation of sulfide by photosynthetic bacteria (Fry et al., 1984).

An explanation for our observed $\delta^{34}S$ pattern may be lower plant incorporation of sulfide-S in the impacted site and also in the higher intertidal zones where we expect that mangrove sediment is relatively more oxidised, and the production of

sulfide may be lower due to lower sulfate reduction. High wood $\delta^{34}S$ values (16.6‰) and S content (0.31%) in the impacted

315   forest may suggest degradation of wood by fungi and/or bacteria that incorporate seawater sulfate-S and increase overall wood $\delta^{34}S$ values and S content. Such $\delta^{34}S$ patterns have been reported in mangroves (Fry and Smith, 2002) and saltmarsh (Currin et al., 1995), where $\delta^{34}S$ values of fresh organic matter evolved during degradation steps and gradually increased towards the $\delta^{34}S$ value of seawater sulfate-S (i.e. 21‰).

4.2 Sediment

320   In healthy mangrove forests, the fate of C fixed by primary producers includes burial within the sediment, atmospheric emissions and outwelling to the ocean (Maher et al., 2018), but how mangrove mortality affects such processes is poorly understood. In most cases, C within in mangrove sediment decreases following forest loss due to degradation with increased CO_2 emissions (Otero et al., 2017; Adame et al., 2018). Lower TOC (%) and higher sediment $\delta^{13}C$ values in the impacted forest (Table 3 and Fig. 4) are probably related to sediment C loss and lower mangrove C inputs (i.e. leaf litter) following the

325   mangrove mortality event. Consistent with this, the sediment N (%) and $\delta^{15}N$ data showed a similar pattern. The surface sediment (0 - 0.5 cm) differed relatively more than the deeper (0.5 to 20 cm) fraction. One explanation for this is that the surface sediment fraction is generally more aerobic, and therefore remineralization of organic matter occurs more rapidly (Burdidge, 2011). Sediment $\delta^{13}C$ and ^{15}N values can increase during degradation of sediment organic matter (Adame and Fry, 2016). This isotope pattern has been reported following mangrove loss (Adame et al., 2018). Changes in sediment C and

330   N may also be associated with root turnover. The MPB $\delta^{13}C$ values significantly differed, with those from the impacted being higher (-21.5 ± 1.3‰) than the unimpacted (-25.2 ± 1.0‰). The higher values probably indicate lower respiratory inputs of CO_2 from mangroves (Maher et al., 2013b). Our findings here are consistent with the finding of Sippo et al. (2019) that changes to oceanic carbon outwelling rates following mangrove loss are likely associated with a gradual loss of sediment carbon; similar to our finding of increased sediment $\delta^{13}C$ values in the impacted site, an isotope effect may have

335   been due to loss of sediment mangrove C or replacement of mangrove peats with marine sediment.

4.3 Fauna

CNS isotopic compositions of consumers including an algae feeder, a grazer and a leaf feeder from the impacted site were consistently more enriched in ^{13}C, ^{15}N and ^{34}S. These differences did not change throughout the three sampling of 2016, 2017 and 2018 (Fig. 5). Consistent with the findings from mangrove leaves, MPB and soil, these data suggested substantial

340   changes in cycling of CNS associated with the mangrove mortality event. Overall, the consumer $\delta^{13}C$ values ranged from -22.9 to -15.2‰ for the unimpacted site, but at the impacted site, consumers were more ^{13}C-enriched (range of -20.0 to -14.0‰), likely due to the loss of ^{13}C-depleted mangrove organic matter. Consumer $\delta^{13}C$ values can change due to changes to available organic matter, altered feeding dependencies as well as changes to organic matter $\delta^{13}C$ values. For example, MPB $\delta^{13}C$ values can change in response to organic matter respiratory inputs. The consumer $\delta^{13}C$ values and their ranges at our

11

345 study site are fairly consistent with the reported mangrove consumer δ13C values elsewhere (e.g. Lee, 2000; Bouillon et al., 2002; Demopoulos et al., 2007). Lower consumer δ13C values near -27‰ are generally associated with mangrove detritus, but in many cases, typical mangrove leaf-eating crab species (i.e. Sesarmidae) can be enriched by about +5‰ from the mangrove detritus (Bui and Lee, 2014). Higher δ13C values of consumers are generally tied to MPB with a typical isotope effect during assimilation, e.g. < ~ 1‰ estimated for small invertebrates (Vander Zanden and Rasmussen, 2001; McCutchan

350 et al., 2003). Our MPB endmember δ13C values of -25.2‰ for the unimpacted site and -21.5‰ for the impacted site did not match with the consumer δ13C values (around -15 to -14‰), suggesting our characterization of MPB endmember δ13C values was incomplete. This is probably because MPB can vary substantially within mangrove ecosystems (Bouillon et al., 2008) and consumers may be preferentially assimilating more 13C enriched fractions of MPB, for example, diatom and/or filamentous cyanobacteria that can range about -15 to -20‰ (Craig, 1953; Fry and Wainright, 1991). The leaf feeder in this

355 study showed δ13C values of about -21 to -18‰ and was substantially enriched compared to mangrove leaves (-27 to -25‰), consistent with the findings of Bui and Lee (2014). This also indicated some additional contributions from other sources such as MPB.

Due to difficulties obtaining representative endmembers, mixing analysis using sampled organic matter was not achieved in

360 this study to quantify feeding dependencies. Alternatively, the consumer data was used to help infer endmembers and assess feeding dependencies, e.g. Riekenberg et al. (2016). POM (-21.1‰) matched with the filter feeders and seemed to be an important food source for the all consumers in both forests. Mangrove leaves (-27 to -25‰) did not seem to be an important source for the consumers with the lowest consumer being -22.9‰ at the unimpacted site and -20.0‰ at the impacted site. The consumers were generally higher than the POM with the highest consumer being -15.2‰ at the unimpacted site and -

365 14.0‰ at the impacted site, suggesting that there was a substantial contribution from more 13C enriched MPB.

Consumer δ34S values were generally higher in the impacted site (range 13.4 to 21.7‰) than in the unimpacted site (range 8.2 to 16‰) suggesting lower sulfate reduction with decreased sulfide inputs at the impacted site. Fixation of sulfate by phytoplankton occurs with a small isotope effect, around 1 to 2‰ (Fry, 2006), so that δ34S values of phytoplankton from the

370 coastal ocean should be close to the seawater sulfate-S value of 21‰. MPB generally have lower δ34S values than phytoplankton, with reported average values near 10‰ for MPB in a mangrove ecosystem (Harada et al., unpublished), likely due to some use of sedimentary sulfide-S (depleted in 34S). Our mangrove leaf δ34S values averaged 13.5‰ for the impacted site and 12.6‰ for the unimpacted site, lower than the seawater sulfate-S. For these reasons, the unimpacted site that had lower consumer δ34S values could be associated with sulfide inputs with some use of mangrove organic matter and

375 MPB, whereas the impacted site that had higher consumer δ34S values are associated more with seawater sulfate. This indicates a change to the S cycling and use of S by plants as well as microbial intermediates in the food web.

12

The consumer δ^{15}N also indicates possible changes to N cycling, with the consumer in the impacted site generally having higher values than those from in the unimpacted site. The higher δ^{15}N may be associated with degradation of organic matter,

380 microbial ^{15}N enrichment in dissolved inorganic N such as ammonium and nitrate during degradation, and ^{15}N enrichment by microbial intermediates in the food web. The high ^{15}N may also indicate lower N fixation inputs that typically show low δ^{15}N values, round 0‰. While the δ^{13}C and δ^{34}S values consistently differed between the two forests during the two-year survey, the δ^{15}N values started showing matches between the two forests in 2018. This may suggest recovery of δ^{15}N status to the background conditions, and/or that the recovery of N may be faster than C and S elements. This may be the case as

385 mangrove ecosystems are generally N limited (Reef et al., 2010), and circulation of N elements is faster than those of C and S elements.

4.4 Compound-specific isotope analysis of amino acids

It is considered that environmental resources such as vascular plants and microalgae have a different δ^{13}C pattern ('fingerprint') in AAs due to differing biosynthesis of AAs (Larsen et al., 2009; Larsen et al., 2013). It is also reported that

390 δ^{13}C patterns are largely unaffected by environmental conditions. For example, $\delta^{13}C_{AA}$ patterns of the marine diatom *Thalassiosira weissflogii* did not respond to changing environmental conditions such as light, salinity, temperature and pH, despite substantial changes in bulk δ^{13}C values (Larsen et al., 2015). A similar isotope pattern was reported for seagrass *Posidonia oceanica* and the giant kelp *Macrocystis pyrifera,* which showed consistent $\delta^{13}C_{AA}$ patterns despite varying season and growth conditions (Larsen et al., 2013). The $\delta^{13}C_{AA}$ patterns in producers, especially those of essential amino acids

395 ($\delta^{13}C_{EAA}$), can reflect consumer tissues with little isotope effect. This occurs because animals obtain EAAs from their diet and EAA fractions are thought to be directly assimilated (McMahon et al., 2010). These general expectations were reasonably met in our $\delta^{13}C_{EAA}$ dataset - that was normalized to means of five EAAs as per Larsen et al. (2009). Normalized $\delta^{13}C_{EAA}$ patterns of our producer samples including mangrove leaves (yellow leaves of *A. marina*) and MPB did not differ between the two sites despite differing environmental conditions and substantial differences in bulk δ^{13}C values (Table 4, Fig

400 6 and Fig S1). Furthermore, the consumer $\delta^{13}C_{EAA}$ patterns also did not differ between the two sites. (Fig. 6 and Fig S1). These findings did not support changes to feeding dependency following mangrove loss but suggested that the overall differences in the consumer bulk δ^{13}C values were most likely driven by differences in the resource organic matter δ^{13}C values e.g. changes to MPB δ^{13}C values that were likely associated with lower mangrove C fixation/respiratory inputs following the mangrove mortality. Furthermore, such findings indicate that the reported substantial change to the mangrove

405 benthic faunal assemblage following the mangrove loss (Harada et al., 2019) was probably driven more by modification of physical habitat structure than changes in the use of food resources.

5 Conclusions

Reporting rare and extreme biological events can be complicated because in many cases they may occur suddenly, therefore drawing comparisons between pre and post event conditions remains a challenge. Our field investigations using traditional

410 ecological techniques combined with SIA - measured the initial dieback and also early recovery of an impacted mangrove ecosystem and compared an adjacent unimpacted reference system. Mangrove seedling and sapling populations that increased during the period from 2016 to 2018 (8 to 32 months after the mortality event) in the impacted site, suggest recovery of the mangrove vegetation. This also suggests that the environmental conditions at the impacted site are still conducive for re-establishment of mangroves, allowing recruitment of seedlings and development of regrowth. However,

415 mangrove leaves collected in the impacted site in 2018 showed relatively higher $\delta^{13}C$ values (-25.8 ± 1.0‰) that are probably associated with continued water stress. Invertebrates from the impacted site representing the feeding types of grazing, leaf feeding, and algae feeding were more enriched in ^{13}C, ^{15}N and ^{34}S relative to those from the unimpacted site. For example, they were more ^{13}C enriched at the impacted site, by 1.7 – 4.1‰ and the difference did not change over the study period. Overall, our stable CNS isotope data supported the hypothesis that changes to biogeochemical processes occur

420 following the mangrove mortality. These changes include lower mangrove C fixation/respiration, lower N fixation and lower sulfate reduction. However, our isotope data did not support the second hypothesis that the isotopic compositions change over time with recovery of mangrove vegetation. Recovery of biogeochemical processes was not evident even after two years, suggesting an ongoing impact of the mortality event. An exception was that N cycle recovery may be occurring faster.

425 Considering that the environmental conditions at the site play an important role in facilitating recolonisation of mangroves, we conceptualise the recovery of the mangrove forest under four different scenarios to give insight into the ecological and biogeochemical consequences of changing forest conditions (Fig. 7): 1) The forest recovers with mangroves being able to recolonise at the site without future perturbations; 2) the forest recovers with future perturbations such as climatic events, for example, mangrove recolonisation is driven by events as such ENSO cycles; 3) the forest does not recover and is

430 transformed into intertidal mudflats; and 4) the forest recovers partially at the site and in a reduced size and/or is recolonised by other plants such as saltmarshes, e.g., mangroves only recolonise in the lower intertidal zone. Each of these scenarios will have a distinct isotopic trajectory for C, N and S. Continued monitoring of the post-dieback forest would be required to predict the long-term trajectory of ecosystem recovery and how on-going climate change and extreme climatic events affect the recovery of mangroves in the impacted region. In such a long-term investigation, SIA is a powerful tool, capable of

435 tracking changes in biogeochemical processes over time. As such, it is of great assistance in ecosystem analyses and detecting the underlying biological mechanisms that drive changes and recovery.

Author contributions. The study was conceptualized by all authors. Writing was led by YH and contributed to by all. Field surveys were executed by DTM, JZS, LCJ, AJB and YH. Data compilation and analysis was coordinated by YH and
440   contributed to by all.

Competing interests. The authors declare no competing interests.

References

Abrantes, K. G., Johnston, R., Connolly, R. M., and Sheaves, M.: Importance of Mangrove Carbon for Aquatic Food Webs in Wet–Dry Tropical Estuaries, Estuaries and Coasts, 38, 383-399, 2015.

Adame, M., and Fry, B.: Source and stability of soil carbon in mangrove and freshwater wetlands of the Mexican Pacific coast, Wetlands ecology and management, 24, 129-137, 2016.

Adame, M., Zakaria, R., Fry, B., Chong, V., Then, Y., Brown, C., and Lee, S. Y..: Loss and recovery of carbon and nitrogen after mangrove clearing, Ocean & Coastal Management, 161, 117-126, 2018.

Asbridge, E., Lucas, R., Ticehurst, C., and Bunting, P.: Mangrove response to environmental change in Australia's Gulf of Carpentaria, Ecology and Evolution, 6, 3523-3539, 2016.

Asbridge, E., Lucas, R., Rogers, K., and Accad, A.: The extent of mangrove change and potential for recovery following severe Tropical Cyclone Yasi, Hinchinbrook Island, Queensland, Australia, Ecology and evolution, 8, 10416-10434, 2018.

Asbridge, E. F., Bartolo, R., Finlayson, C. M., Lucas, R. M., Rogers, K., and Woodroffe, C. D.: Assessing the distribution and drivers of mangrove dieback in Kakadu National Park, northern Australia, Estuarine, Coastal and Shelf Science, 106353, 2019.

Bernardino, A. F., Gomes, L. E. D. O., Hadlich, H. L., Andrades, R., and Correa, L. B.: Mangrove clearing impacts on macrofaunal assemblages and benthic food webs in a tropical estuary, Marine Pollution Bulletin, 126, 228-235, 2018.

Bouillon, S., Koedam, N., Raman, A., and Dehairs, F.: Primary producers sustaining macro-invertebrate communities in intertidal mangrove forests, Oecologia, 130, 441-448, 2002.

Bouillon, S., Connolly, R. M., and Lee, S. Y.: Organic matter exchange and cycling in mangrove ecosystems: Recent insights from stable isotope studies, Journal of Sea Research, 59, 44-58, 2008.

Bui, T. H. H., and Lee, S. Y.: Does 'You Are What You Eat' Apply to Mangrove Grapsid Crabs?, PLOS ONE, 9, e89074, 2014.

Burdige, D.: 5.09 Estuarine and coastal sediments–coupled biogeochemical cycling, Treatise on Estuarine and Coastal Science, 5, 279-308, 2011.

Cahoon, D. R., Hensel, P., Rybczyk, J., McKee, K. L., Proffitt, C. E., and Perez, B. C.: Mass tree mortality leads to mangrove peat collapse at Bay Islands, Honduras after Hurricane Mitch, Journal of Ecology, 91, 1093-1105, 2003.

Cordell, S., Goldstein, G., Meinzer, F. C., and Handley, L. L.: Allocation of nitrogen and carbon in leaves of Metrosideros polymorpha regulates carboxylation capacity and $\delta^{13}C$ along an altitudinal gradient, Functional Ecology, 13, 811-818, 1999.

Coumou, D., and Rahmstorf, S.: A decade of weather extremes, Nature Climate Change, 2, 491-496, 2012.

Craig, H.: The geochemistry of the stable carbon isotopes, Geochimica et Cosmochimica Acta, 3, 53-92, 1953.

Currin, C. A., Newell, S. Y., and Paerl, H.: The role of standing dead Spartina alterniflora and benthic microalgae in salt marsh food webs: considerations based on multiple stable isotope analysis, Marine Ecology Progress Series, 121, 99-116, 1995.

Demopoulos, A. W., Fry, B., and Smith, C. R.: Food web structure in exotic and native mangroves: a Hawaii–Puerto Rico comparison, Oecologia, 153, 675-686, 2007.

485   Docherty, G., Jones, V., and Evershed, R. P.: Practical and theoretical considerations in the gas chromatography/combustion/isotope ratio mass spectrometry δ^{13}C analysis of small polyfunctional compounds, Rapid Communications in Mass Spectrometry, 15, 730-738, 2001.

Dore, J. E., Brum, J. R., Tupas, L. M., and Karl, D. M.: Seasonal and interannual variability in sources of nitrogen supporting export in the oligotrophic subtropical North Pacific Ocean, Limnology and Oceanography, 47, 1595-1607, 2002.

490   Duke, N. C., Kovacs, J. M., Griffiths, A. D., Preece, L., Hill, D. J., Van Oosterzee, P., Mackenzie, J., Morning, H. S., and Burrows, D.: Large-scale dieback of mangroves in Australia's Gulf of Carpentaria: a severe ecosystem response, coincidental with an unusually extreme weather event, Marine and Freshwater Research, 68, 1816-1829, 2017.

Farquhar, G. D., Ehleringer, J. R., and Hubick, K. T.: Carbon isotope discrimination and photosynthesis, Annual review of plant biology, 40, 503-537, 1989.

495   Fogel, M., Wooller, M., Cheeseman, J., Smallwood, B., Roberts, Q., Romero, I., and Meyers, M. J.: Unusually negative nitrogen isotopic compositions (δ^{15}N) of mangroves and lichens in an oligotrophic, microbially-influenced ecosystem, Biogeosciences, 5, 1693-1704, 2008.

Fry, B., Scalan, R. S., Winters, J. K., and Parker, P. L.: Sulphur uptake by salt grasses, mangroves, and seagrasses in anaerobic sediments, Geochimica et Cosmochimica Acta, 46, 1121-1124, 1982.

500   Fry, B., Gest, H., and Hayes, J. M.: Isotope effects associated with the anaerobic oxidation of sulfide by the purple photosynthetic bacterium, Chromatium vinosum, FEMS Microbiology Letters, 22, 283-287, 1984.

Fry, B., Ruf, W., Gest, H., and Hayes, J. M.: Sulfur isotope effects associated with oxidation of sulfide by O_2 in aqueous solution, Chemical Geology: Isotope Geoscience section, 73, 205-210, 1988.

Fry, B., and Wainright, S. C.: Diatom sources of ^{13}C-rich carbon in marine food webs, Marine Ecology Progress Series, 149-
505   157, 1991.

Fry, B., Bern, A. L., Ross, M. S., and Meeder, J. F.: δ^{15}N Studies of Nitrogen Use by the Red Mangrove, Rhizophora mangle L. in South Florida, Estuarine, Coastal and Shelf Science, 50, 291-296, 2000.

Fry, B., and Smith, T. J.: Stable isotope studies of red mangroves and filter feeders from the Shark River estuary, Florida, Bulletin of Marine Science, 70, 871-890, 2002.

510   Fry, B.: Stable isotope ecology, Springer, 2006.

Fry, B., and Cormier, N.: Chemical Ecology of Red Mangroves, Rhizophora mangle, in the Hawaiian Islands1, Pacific Science, 65, 219-235, 2011.

Harada, Y., Fry, B., Lee, S. Y., Maher, D. T., Sippo, J. Z., and Connolly, R. M.: Stable isotopes indicate ecosystem restructuring following climate-driven mangrove dieback, Limnology and Oceanography, 2019.

515   Harada, Y., and Lee, S. Y.: Foraging behavior of the mangrove sesarmid crab Neosarmatium trispinosum enhances food intake and nutrient retention in a low-quality food environment, Estuarine, Coastal and Shelf Science, 174, 41-48, 2016.

Harris, R. M. B., Beaumont, L. J., Vance, T. R., Tozer, C. R., Remenyi, T. A., Perkins-Kirkpatrick, S. E., Mitchell, P. J., Nicotra, A. B., McGregor, S., Andrew, N. R., Letnic, M., Kearney, M. R., Wernberg, T., Hutley, L. B., Chambers, L. E., Fletcher, M. S., Keatley, M. R., Woodward, C. A., Williamson, G., Duke, N. C., and Bowman, D. M. J. S.: Biological

520 responses to the press and pulse of climate trends and extreme events, Nature Climate Change, 8, 579-587, 2018.

Harris, T., Hope, P., Oliver, E., Smalley, R., Arblaster, J., Holbrook, N., Duke, N., Pearce, K., Braganza, K., and Bindoff, N.: Climate drivers of the 2015 Gulf of Carpentaria mangrove dieback, Earth Systems and Climate Change Hub Technical Report No, 2, 2017.

Hayes, M. A., Jesse, A., Welti, N., Tabet, B., Lockington, D., and Lovelock, C. E.: Groundwater enhances above-ground

525 growth in mangroves, Journal of Ecology, 107, 1120-1128, 2019.

Hughes, T. P., Kerry, J. T., Álvarez-Noriega, M., Álvarez-Romero, J. G., Anderson, K. D., Baird, A. H., Babcock, R. C., Beger, M., Bellwood, D. R., Berkelmans, R., Bridge, T. C., Butler, I. R., Byrne, M., Cantin, N. E., Comeau, S., Connolly, S. R., Cumming, G. S., Dalton, S. J., Diaz-Pulido, G., Eakin, C. M., Figueira, W. F., Gilmour, J. P., Harrison, H. B., Heron, S. F., Hoey, A. S., Hobbs, J. P. A., Hoogenboom, M. O., Kennedy, E. V., Kuo, C. Y., Lough, J. M., Lowe, R. J., Liu, G.,

530 McCulloch, M. T., Malcolm, H. A., McWilliam, M. J., Pandolfi, J. M., Pears, R. J., Pratchett, M. S., Schoepf, V., Simpson, T., Skirving, W. J., Sommer, B., Torda, G., Wachenfeld, D. R., Willis, B. L., and Wilson, S. K.: Global warming and recurrent mass bleaching of corals, Nature, 543, 373-377, 2017.

Imbert, D., Rousteau, A., and Scherrer, P.: Ecology of mangrove growth and recovery in the Lesser Antilles: state of knowledge and basis for restoration projects, Restoration Ecology, 8, 230-236, 2000.

535 Ishikawa, N. F., Chikaraishi, Y., Takano, Y., Sasaki, Y., Takizawa, Y., Tsuchiya, M., Tayasu, I., Nagata, T., and Ohkouchi, N.: A new analytical method for determination of the nitrogen isotopic composition of methionine: Its application to aquatic ecosystems with mixed resources, Limnology and Oceanography: Methods, 16, 607-620, 2018.

Kaplan, I., and Rittenberg, S.: Microbiological fractionation of sulphur isotopes, Microbiology, 34, 195-212, 1964.

Kelleway, J. J., Mazumder, D., Baldock, J. A., and Saintilan, N.: Carbon isotope fractionation in the mangrove Avicennia

540 marina has implications for food web and blue carbon research, Estuarine, Coastal and Shelf Science, 205, 68-74, 2018.

Kling, G. W., Fry, B., and O'Brien, W. J.: Stable Isotopes and Planktonic Trophic Structure in Arctic Lakes, Ecology, 73, 561-566, 1992.

Krauss, K. W., and Osland, M. J.: Tropical cyclones and the organization of mangrove forests: a review, Annals of Botany, 2019.

545 Larsen, T., Taylor, D. L., Leigh, M. B., and O'Brien, D. M.: Stable isotope fingerprinting: a novel method for identifying plant, fungal, or bacterial origins of amino acids, Ecology, 90, 3526-3535, 2009.

Larsen, T., Wooller, M. J., Fogel, M. L., and O'Brien, D. M.: Can amino acid carbon isotope ratios distinguish primary producers in a mangrove ecosystem?, Rapid Communications in Mass Spectrometry, 26, 1541-1548, 2012.

Larsen, T., Ventura, M., Andersen, N., O'Brien, D. M., Piatkowski, U., and McCarthy, M. D.: Tracing Carbon Sources

550 through Aquatic and Terrestrial Food Webs Using Amino Acid Stable Isotope Fingerprinting, PLoS ONE, 8, e73441, 2013.

Larsen, T., Bach, L. T., Salvatteci, R., Wang, Y. V., Andersen, N., Ventura, M., and McCarthy, M. D.: Assessing the potential of amino acid ^{13}C patterns as a carbon source tracer in marine sediments: effects of algal growth conditions and sedimentary diagenesis, Biogeosciences, 12, 4979-4992, 2015.

Lee, S. Y.: Carbon dynamics of Deep Bay, eastern Pearl River estuary, China. II: Trophic relationship based on carbon-and
555 nitrogen-stable isotopes, Marine Ecology Progress Series, 205, 1-10, 2000.

Lin, G., and Sternberg, L.: Differences in morphology, carbon isotope ratios, and photosynthesis between scrub and fringe mangroves in Florida, USA, Aquatic Botany, 42, 303-313, 1992a.

Lin, G., and Sternberg, L.: Effect of growth form, salinity, nutrient and sulfide on photosynthesis, carbon isotope discrimination and growth of red mangrove (Rhizophora mangle L.), Functional Plant Biology, 19, 509-517, 1992b.

560 Lovelock, C. E., Feller, I. C., Reef, R., Hickey, S., and Ball, M. C.: Mangrove dieback during fluctuating sea levels, Scientific Reports, 7, 1680, 2017.

Maher, D. T., Santos, I. R., Golsby-Smith, L., Gleeson, J., and Eyre, B. D.: Groundwater-derived dissolved inorganic and organic carbon exports from a mangrove tidal creek: The missing mangrove carbon sink?, Limnology and Oceanography, 58, 475-488, 2013a.

565 Maher, D. T., Santos, I. R., Leuven, J. R. F. W., Oakes, J. M., Erler, D. V., Carvalho, M. C., and Eyre, B. D.: Novel Use of Cavity Ring-down Spectroscopy to Investigate Aquatic Carbon Cycling from Microbial to Ecosystem Scales, Environmental Science & Technology, 47, 12938-12945, 2013b.

Maher, D. T., Santos, I. R., Schulz, K. G., Call, M., Jacobsen, G. E., and Sanders, C. J.: Blue carbon oxidation revealed by radiogenic and stable isotopes in a mangrove system, Geophysical Research Letters, 44, 4889-4896, 2017.

570 Maher, D. T., Call, M., Santos, I. R., and Sanders, C. J.: Beyond burial: lateral exchange is a significant atmospheric carbon sink in mangrove forests, Biology Letters, 14, 20180200, 2018.

Mbense, S., Rajkaran, A., Bolosha, U., and Adams, J.: Rapid colonization of degraded mangrove habitat by succulent salt marsh, South African journal of botany, 107, 129-136, 2016.

McCutchan, J. H., Lewis Jr, W. M., Kendall, C., and McGrath, C. C.: Variation in trophic shift for stable isotope ratios of
575 carbon, nitrogen, and sulfur, Oikos, 102, 378-390, 2003.

McKee, K. L., Feller, I. C., Popp, M., and Wanek, W.: Mangrove isotopic (δ^{15}N and δ^{13}C) fractionation across a nitrogen vs. phosphorus limitation gradient, Ecology, 83, 1065-1075, 2002.

McKee, K. L., Rooth, J. E., and Feller, I. C.: Mangrove recruitment after forest disturbance is facilitated by herbaceous species in the Caribbean, Ecological Applications, 17, 1678-1693, 2007.

580 McMahon, K. W., Fogel, M. L., Elsdon, T. S., and Thorrold, S. R.: Carbon isotope fractionation of amino acids in fish muscle reflects biosynthesis and isotopic routing from dietary protein, Journal of Animal Ecology, 79, 1132-1141, 2010.

Milbrandt, E., Greenawalt-Boswell, J., Sokoloff, P., and Bortone, S.: Impact and response of Southwest Florida mangroves to the 2004 hurricane season, Estuaries and Coasts, 29, 979-984, 2006.

Ohkouchi, N., Chikaraishi, Y., Close, H. G., Fry, B., Larsen, T., Madigan, D. J., McCarthy, M. D., McMahon, K. W.,
585 Nagata, T., Naito, Y. I., Ogawa, N. O., Popp, B. N., Steffan, S., Takano, Y., Tayasu, I., Wyatt, A. S. J., Yamaguchi, Y. T.,
and Yokoyama, Y.: Advances in the application of amino acid nitrogen isotopic analysis in ecological and biogeochemical
studies, Organic Geochemistry, 113, 150-174, 2017.

Okada, N., and Sasaki, A.: Characteristics of Sulfur Uptake by Mangroves: an Isotopic Study, Tropics, 4, 201-210, 1995.

Okada, N., and Sasaki, A.: Sulfur isotopic composition of mangroves, Isotopes in environmental and health studies, 34, 61-
590 65, 1998.

Otero, X. L., Méndez, A., Nóbrega, G. N., Ferreira, T. O., Santiso-Taboada, M. J., Meléndez, W., and Macías, F.: High
fragility of the soil organic C pools in mangrove forests, Marine Pollution Bulletin, 119, 460-464, 2017.

Rashid, S., Biswas, S. R., Böcker, R., and Kruse, M.: Mangrove community recovery potential after catastrophic
disturbances in Bangladesh, Forest Ecology and Management, 257, 923-930, 2009.

595 Raven, M. R., Fike, D. A., Gomes, M. L., and Webb, S. M.: Chemical and isotopic evidence for organic matter sulfurization
in redox gradients around mangrove roots, Frontiers in Earth Science, 7, 98, 2019.

Reef, R., Feller, I. C., and Lovelock, C. E.: Nutrition of mangroves, Tree Physiology, 30, 1148-1160, 2010.

Riekenberg, P. M., Carney, R. S., and Fry, B.: Trophic plasticity of the methanotrophic mussel Bathymodiolus childressi in
the Gulf of Mexico, Marine Ecology Progress Series, 547, 91-106, 2016.

600 Santini, N. S., Reef, R., Lockington, D. A., and Lovelock, C. E.: The use of fresh and saline water sources by the mangrove
Avicennia marina, Hydrobiologia, 745, 59-68, 2015.

Sasmito, S. D., Kuzyakov, Y., Lubis, A. A., Murdiyarso, D., Hutley, L. B., Bachri, S., Friess, D. A., Martius, C., Borchard,
N.: Organic carbon burial and sources in soils of coastal mudflat and mangrove ecosystems, CATENA, 187, 104414, 2020.

Sherman, R. E., Fahey, T. J., and Martinez, P.: Hurricane Impacts on a Mangrove Forest in the Dominican Republic:
605 Damage Patterns and Early Recovery 1, Biotropica, 33, 393-408, 2001.

Silliman, B. R., van de Koppel, J., Bertness, M. D., Stanton, L. E., and Mendelssohn, I. A.: Drought, Snails, and Large-Scale
Die-Off of Southern U.S. Salt Marshes, Science, 310, 1803-1806, 2005.

Sippo, J. Z., Lovelock, C. E., Santos, I. R., Sanders, C. J., and Maher, D. T.: Mangrove mortality in a changing climate: An
overview, Estuarine, Coastal and Shelf Science, 215, 241-249, 2018.

610 Sippo, J. Z., Maher, D. T., Schulz, K. G., Sanders, C. J., McMahon, A., Tucker, J., and Santos, I. R.: Carbon outwelling
across the shelf following a massive mangrove dieback in Australia: Insights from radium isotopes, Geochimica et
Cosmochimica Acta, 253, 142-158, 2019.

Sjöling, S., Mohammed, S. M., Lyimo, T. J., and Kyaruzi, J. J.: Benthic bacterial diversity and nutrient processes in
mangroves: impact of deforestation, Estuarine, Coastal and Shelf Science, 63, 397-406, 2005.

615 Smallwood, B. J., Wooller, M. J., Jacobson, M. E., and Fogel, M. L.: Isotopic and molecular distributions of biochemicals
from fresh and buried Rhizophora mangle leaves, Geochemical Transactions, 4, 38, 2003.

Smith, T. J., Robblee, M. B., Wanless, H. R., and Doyle, T. W.: Mangroves, hurricanes, and lightning strikes: assessment of Hurricane Andrew suggests an interaction across two differing scales of disturbance, BioScience, 44, 256-262, 1994.

Stott, P.: How climate change affects extreme weather events, Science, 352, 1517-1518, 2016.

620   Sweetman, A., Middelburg, J., Berle, A., Bernardino, A., Schander, C., Demopoulos, A., and Smith, C.: Impacts of exotic mangrove forests and mangrove deforestation on carbon remineralization and ecosystem functioning in marine sediments, Biogeosciences, 7, 2129-2145, 2010.

Thomson, J. A., Burkholder, D. A., Heithaus, M. R., Fourqurean, J. W., Fraser, M. W., Statton, J., and Kendrick, G. A.: Extreme temperatures, foundation species, and abrupt ecosystem change: an example from an iconic seagrass ecosystem, 625   Global Change Biology, 21, 1463-1474, 2015.

Tomlinson, P. B.: The botany of mangroves, Cambridge University Press, 2016.

Trust, B., and Fry, B.: Stable sulphur isotopes in plants: a review, Plant, Cell & Environment, 15, 1105-1110, 1992.

Vander Zanden, M. J., and Rasmussen, J. B.: Variation in δ^{15}N and δ^{13}C trophic fractionation: Implications for aquatic food web studies, Limnology and Oceanography, 46, 2061-2066, 2001.

630   Wernberg, T., Bennett, S., Babcock, R. C., de Bettignies, T., Cure, K., Depczynski, M., Dufois, F., Fromont, J., Fulton, C. J., Hovey, R. K., Harvey, E. S., Holmes, T. H., Kendrick, G. A., Radford, B., Santana-Garcon, J., Saunders, B. J., Smale, D. A., Thomsen, M. S., Tuckett, C. A., Tuya, F., Vanderklift, M. A., and Wilson, S.: Climate-driven regime shift of a temperate marine ecosystem, Science, 353, 169-172, 2016.

Werth, M., Mehltreter, K., Briones, O., and Kazda, M.: Stable carbon and nitrogen isotope compositions change with leaf 635   age in two mangrove ferns, Flora-Morphology, Distribution, Functional Ecology of Plants, 210, 80-86, 2015.

Table 1. Analyses conducted for samples from each field campaign (x = analysed).

Analysis	2016 (8 months after dieback)	2017 (20 months after dieback)	2018 (32 months after dieback)
Mangrove seedling count	x	x	x
Bulk SIA invertebrates	x	x	x
Bulk SIA mangrove			x
Bulk SIA sediment			x
CSIA invertebrates		x	

640   **Table 2.** Elemental and isotopic compositions of the mangrove *A. marina* (mean, SD) in 2018, 32 months after the dieback.

Tissue type	Forest	%C	%N	%S	$\delta^{13}C$, ‰	$\delta^{15}N$, ‰	$\delta^{34}S$, ‰	n
Green leaf	Unimpacted	39.3, 1.7	1.75, 0.37	0.54, 0.23	-28.4, 1.5	4.4, 0.8	12.6, 5.6	15
	Impacted	40.0, 1.6	1.82, 0.45	0.73, 0.14	-25.8, 1.0	4.3, 1.9	13.5, 5.4	15
Yellow leaf	Unimpacted	41.6, 2.2	0.67, 0.23	1.18, 0.47	-26.4, 1.3	6.5, 1.1	14.6, 7.7	3
	Impacted	41.9, 1.0	0.52, 0.05	1.18, 0.38	-26.2, 0.6	7.4, 0.2	12.5, 2.8	3
Wood	Unimpacted	42.6, 3.0	0.38, 0.27	0.04, 0.01	-24.8, 1.8	6.1, 2.0	-	2
	Impacted	39.9, 5.7	0.40, 0.16	0.31, 0.37	-24.9, 1.0	4.7, 1.0	16.6	2

Table 3. Elemental and isotopic compositions of sediment in 2018, 32 months after the dieback (mean, SD).

	Forest/site	%TOC	%TN	δ^{13}C, ‰	δ^{15}N, ‰	n
Mangrove forest, 0 to 0.5 cm	Unimpacted	2.02, 1.16	0.15, 0.06	-24.3, 1.2	2.0, 0.5*	15
	Impacted	1.06, 0.37	0.09, 0.03	-21.8, 1.0	2.8, 0.6*	15
Mangrove forest, 0.5 to 20 cm	Unimpacted	1.83, 0.73	0.12, 0.04	-25.2, 0.9	1.7, 0.5*	6
	Impacted	1.29, 0.55	0.09, 0.03	-24.4, 0.5	1.7, 0.3*	6
Mudflat, 0 to 0.5 cm	Unimpacted	1.02, 0.08	0.11, 0.01	-21.8, 0.8	-	3
	Impacted	0.58, 0.18	0.07, 0.02	-21.2, 0.9	-	3
Saltpan, 0 to 0.5 cm	Unimpacted	1.87, 2.03	0.19, 0.24	-18.9, 1.7	-	4
	Impacted	0.83, 0.07	0.07, 0.01	-20.8, 0.7	-	4
Offshore, 0 to 0.5 cm	1km offshore	0.70, 0.27	0.08, 0.03	-21.8, 1.1	-	5
POM	1km offshore	-	-	-21.1, 1.5	3.6, 2.1	3
MPB	Unimpacted	-	-	-25.2, 1.0	-	6
	Impacted	-	-	-21.5, 1.3	-	6

*values were taken from Harada et al. (2019)

645 **Table 4**. Bulk $\delta^{13}C$ values, mean $\delta^{13}C$ values of five EAAs (‰) and differences (Δ, ‰) between the two forests in 2017, 20 months after the dieback (mean, SD).

Group	Taxa	Forest	Bulk $\delta^{13}C$, ‰	Mean $\delta^{13}C$ of five EAAs, ‰	n	Δ Bulk $\delta^{13}C$, ‰	Δ Mean $\delta^{13}C$ of five EAAs, ‰	Permanova p value
Algal feeder	*Tubuca signata*	Unimpacted	-17.1, 1.4	-21.9, 1.5	3	1.7	1.4	0.90
		Impacted	-15.4, 1.4	-20.5, 1.8	3			
Leaf feeder	*Parasesarma / Episesarma*	Unimpacted	-21.4, 1.5	-25.3, 1.6	3	3.1	1.4	0.40
		Impacted	-18.3, 0.2	-23.9, 0.1	2			
Grazer	*Telescopium telescopium*	Unimpacted	-18.2, 1.9	-24.0, 1.8	3	1.5	1.8	0.80
		Impacted	-16.7, 1.3	-22.2, 1.1	3			
Filter feeder	*Crassostrea* (oyster)	Unimpacted	-19.3, 0.4	-22.8, 0.2	2	0.3	0.1	0.33
		Impacted	-19.0, 0.8	-22.9, 0.3	2			
Mangrove	*Avicennia marina*	Unimpacted	-26.7, 2.2	-28.8, 0.6	2	1.3	1.8	0.67
		Impacted	-25.4, 0.1	-27.0, 0.3	2			
MPB		Unimpacted	-25.4, 0.8	-27.4	1	4.5	6.7	-
		Impacted	-20.9, 1.2	-20.7	1			
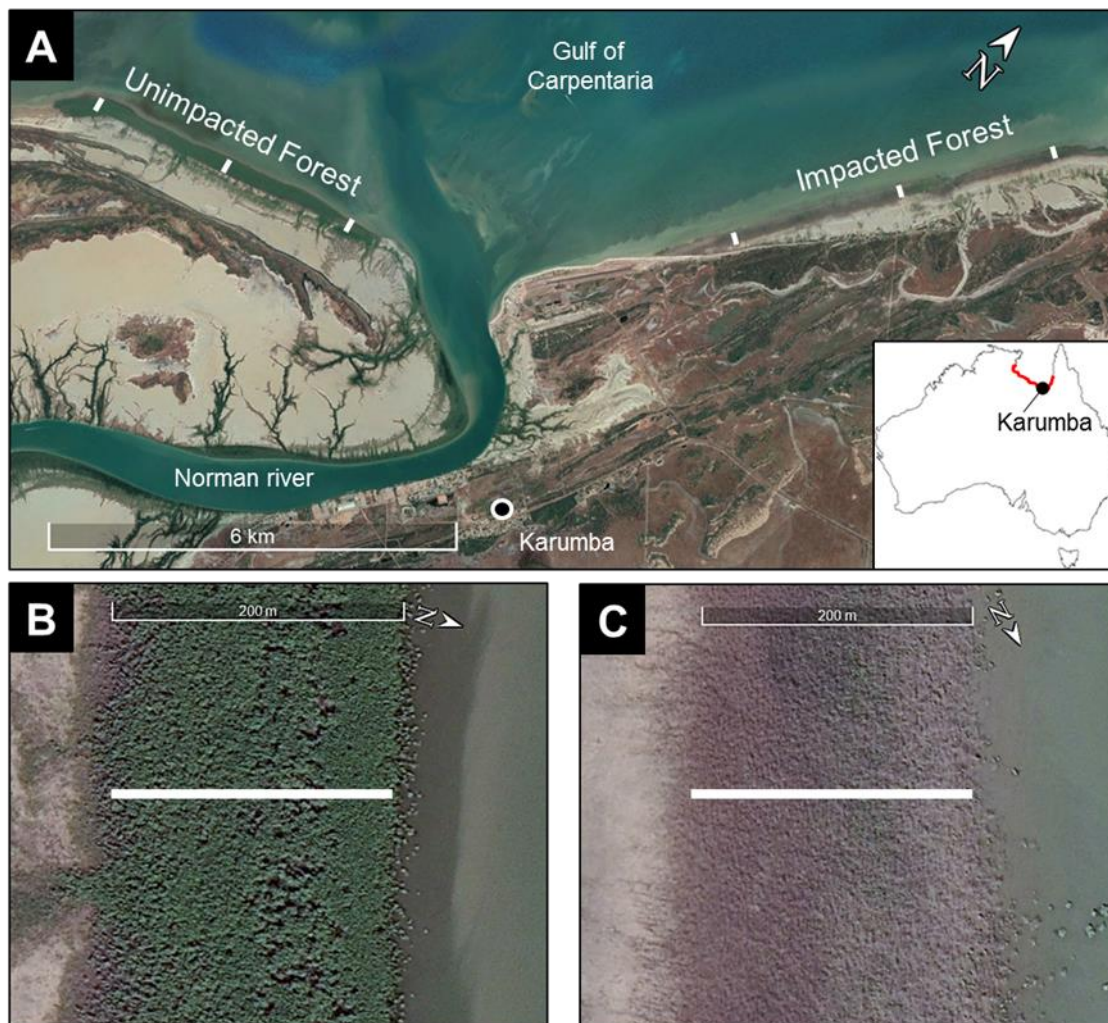
Figure 1. The study location at Karumba in the Gulf of Carpentaria, Queensland, Australia (-17.435572S, 140.844766E;
image provided by © Google Earth). (A) Three sampling transects within the unimpacted reference site and three within
the impacted site (shown as a white line). (B, C) Representative transects from the unimpacted (B) and impacted (C) sites.
Each transect was approximately 200m. Samples were collected along each transect from higher to lower intertidal
zones. Red indicated mass dieback region.
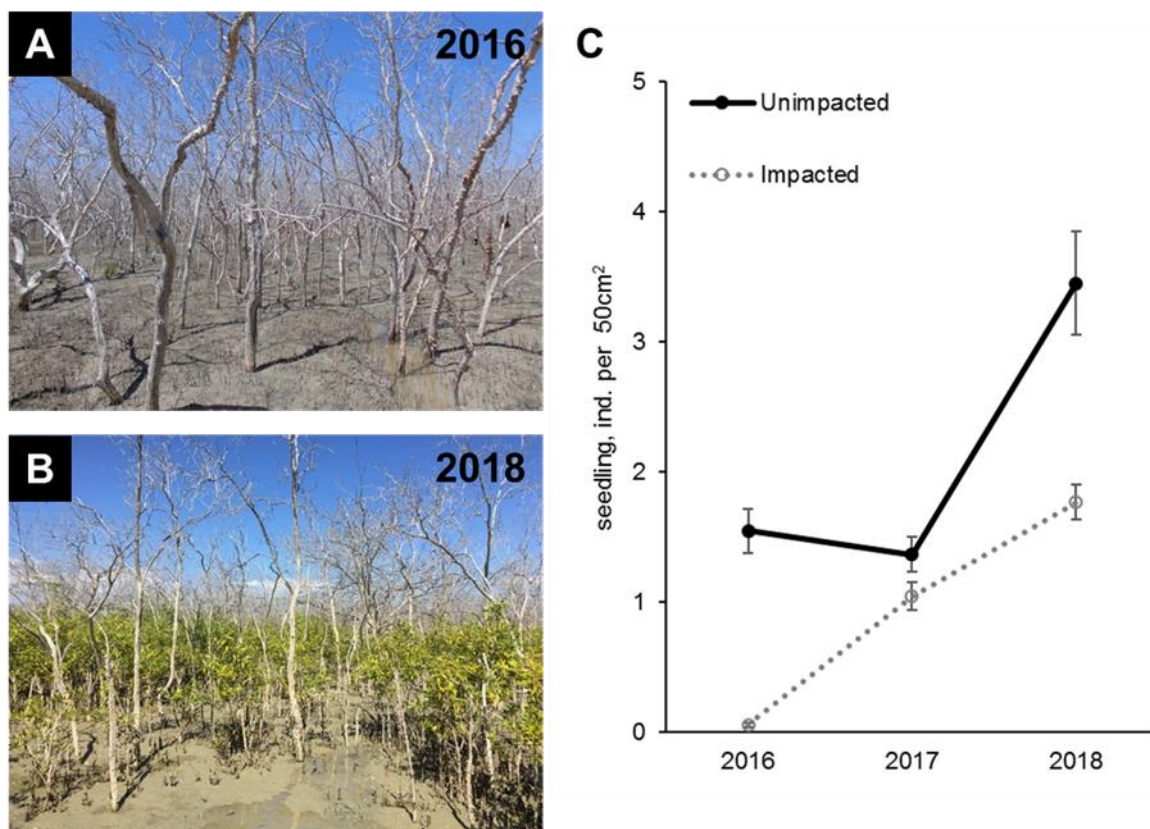
Figure 2. Recovery of mangrove vegetation at the impacted site during a two-year period from 2016 to 2018 (A and B; approx. 8 and 32 months, respectively after the dieback event). Seedling and sampling populations of mangrove species (mostly, *A. marina*) significantly increased in the impacted site (C).

660
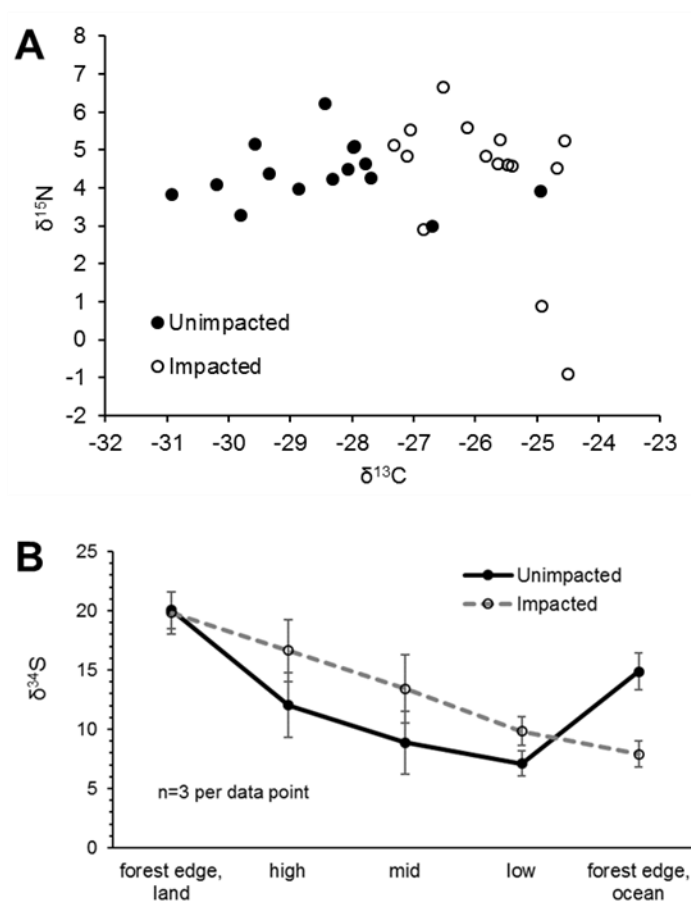
Figure 3. CNS isotopic compositions of green leaves of *A. marina* from the unimpacted and impacted sites. All samples were collected in 2018, 32 months after the dieback. (A) Leaf $\delta^{13}C$ and $\delta^{15}N$ values. (B) Leaf $\delta^{34}S$ values across the intertidal zones. Error values are SE.

665
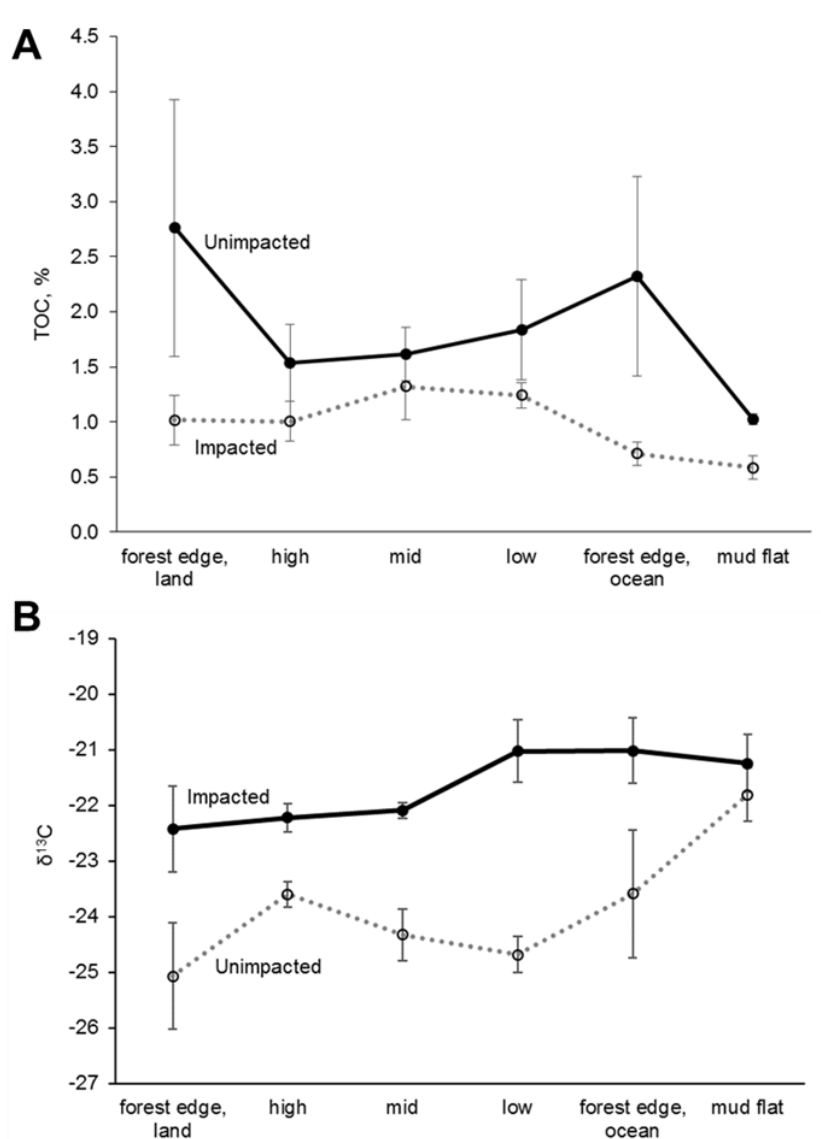
Figure 4. C elemental and isotopic compositions of surface (< 0.5 cm) sediment along the unimpacted reference transects vs impacted transects (n=3 per data point). All samples were collected in 2018, 32 months after the dieback. Error values are SE. (A) Sediment TOC, %. (B) Sediment $\delta^{13}C$ values, ‰.

670
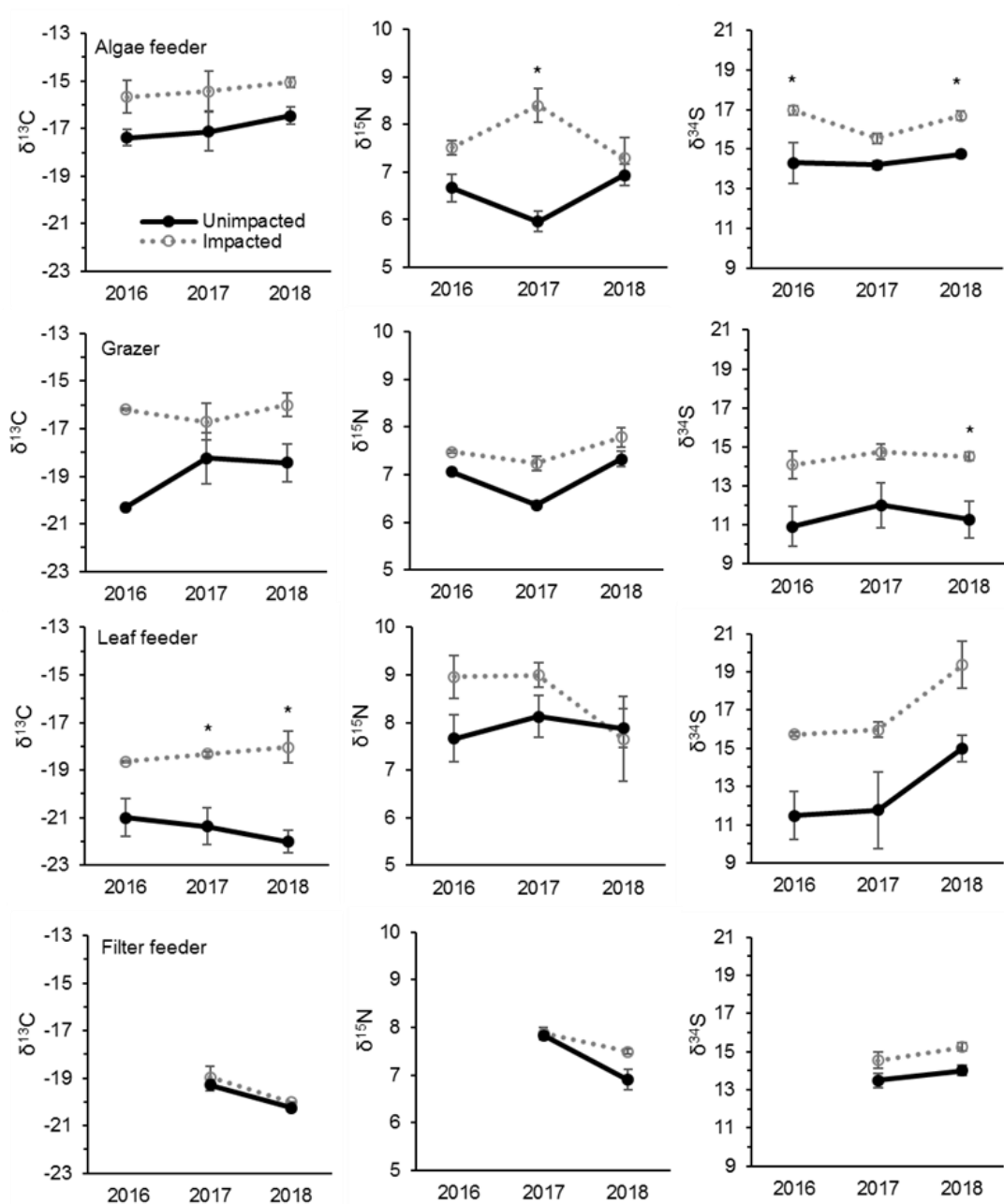
Figure 5. Changes in CNS isotopic compositions of mangrove macrofaunal groups with four different feeding modes from 2016, 2017 and 2018 (i.e. 8, 20 and 32 months after the event) between the unimpacted reference and impacted mangrove forest sites. Error bars are ± SE (n=2 to 6 per data point). (*) indicates a significant difference in the year. Mean ± SE values and sample sizes are also provided in Table S1.
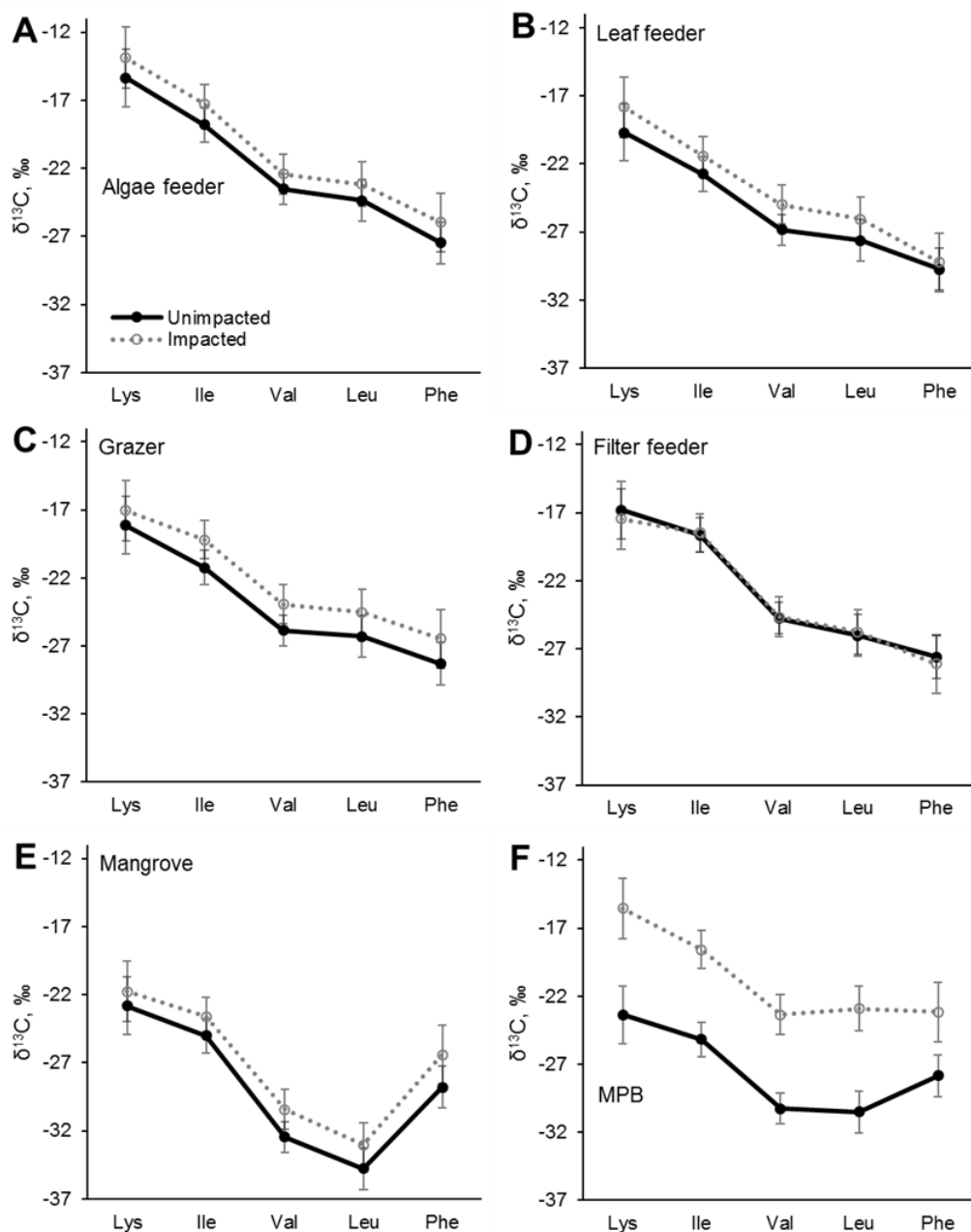
Figure 6. C isotopic compositions in essential amino acids (EAAs) for four mangrove consumer groups and resources including mangrove leaves (*A. marina*) and MPB from the unimpacted and impacted mangrove sites during 2017 (20 months after the dieback). While there are clear offsets in individual $\delta^{13}C_{EAA}$ values between the two forests, normalized $\delta^{13}C_{EAA}$ fingerprint patterns as per Larsen (2009) shown in Fig S1 did not differ (PERMANOVA p > 0.05, Table 3). Error bars show ± SD.

Disturbance legacies of the forest dieback

Forest dieback due to extreme climatic events (impacted)
- $\delta^{13}C$ - weak C_3 plants signal (due to loss of mangroves)
- $\delta^{15}N$ - Moderate to high (due to degradation and lower N fixation)
- $\delta^{34}S$ - Moderate to high (lower sulfate reduction with a strong seawater sulfate signal)

Healthy mangrove ecosystem (background)
- $\delta^{13}C$ - strong C_3 plants signal
- $\delta^{15}N$ - Low to moderate (high N fixation)
- $\delta^{34}S$ - Low to moderate (high sulfate reduction)

Predicted recovery scenarios with isotopic trajectories

(1) Recovery with no future perturbations
- Environmental conditions allow recolonisation
- Recovery of $\delta^{13}C$, $\delta^{15}N$ and $\delta^{34}S$ to the background
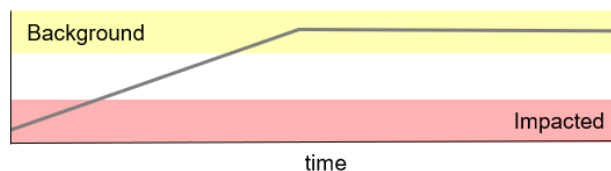
(2) Recovery with future perturbations
- Mangrove recolonisation and recovery of $\delta^{13}C$, $\delta^{15}N$ and $\delta^{34}S$ driven by perturbations e.g. ENSO cycles
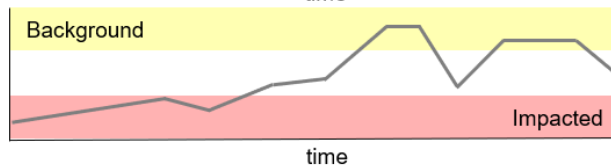
(3) Habitat becomes unsuitable for recolonisation
- Conditions not allow recolonisation e.g. due to extreme climatic events
- Transformed into intertidal mudflats
- No recovery of isotopes
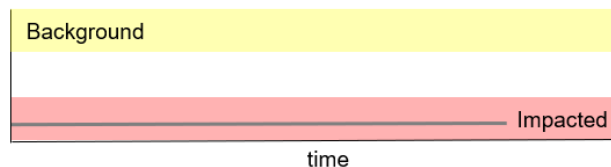
(4) Incomplete recovery
- Reduced habitat size and/or recolonised by other plants such as saltmarshes
- Incomplete recovery of $\delta^{13}C$, $\delta^{15}N$ and $\delta^{34}S$
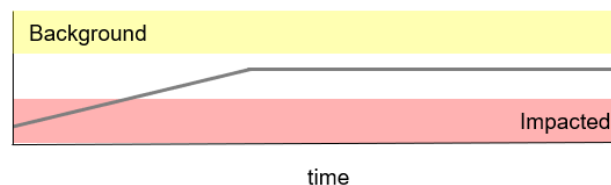
Figure 7. A conceptual diagram showing the ecological and biogeochemical legacy of the mangrove forest dieback in the Gulf of Carpentaria and four predicted recovery scenarios of the mangrove ecosystem with isotopic trajectories.